The 14th World Conference on Earthquake Engineering
October 12-17, 2008, Beijing, China

TESTING OF Cu-BASED SMA SEISMIC ENERGY DISSIPATION DEVICES

M.O. Moroni[1], R. Herrera[2] and M. Sarrazin[3]

[1] *Associate Professor, Dept. of Civil Engineering , University of Chile, Santiago, Chile*
[2] *Assistant Professor, Dept. of Civil Engineering, University of Chile, Santiago, Chile*
[3] *Professor, Dept. of Civil Engineering, University of Chile, Santiago, Chile*
Email: mmoroni@ing.uchile.cl

ABSTRACT :

This paper presents the results of a study on Cu-based shape memory alloys (SMA) elements for energy dissipation in connections under earthquake excitation. The elements include round bars for use as mechanical connectors and plates for ADAS-type energy dissipation devices. The goal of the study is to determine the behaviour of elements with full-scale dimensions, and evaluate possible scale effects on their shape memory or superelastic properties. Two nominal compositions of CuZnAl were used. The study of both compositions in parallel is of interest because of the large energy dissipation capacity of one and the self-centering capability of the other. Both materials may be combined to optimize the behaviour of connections that include elements made of these alloys. Bars of different diameters were fabricated using extrusion and hot-rolling. The mechanical properties (stiffness, martensitic transformation stress, tensile strength, ultimate strain) and equivalent damping of these bars were experimentally determined and their dependency on type, amplitude and frequency of excitation, and working temperature was studied. In addition, four annealed martensite plates (15x12x1 cm) were tested under cyclic out-of-plane flexure. Stable cycles and limited residual deformations were observed up to 20% drift. Equivalent damping ratio increased with larger drift, reaching a maximum of 8% for a 20% drift.

KEYWORDS: Shape Memory Alloy, Dissipation Devices, Superelasticity

1. INTRODUCTION

Shape memory alloys (SMAs) are materials that can exhibit large strains under loading-unloading process without residual deformation. Depending on the working temperature, the removal of deformations induced by stress may require unloading and heating (shape memory effect) or simply unloading (superelasticity). SMA is composed of a high-temperature parent phase, austenite or phase ß, with high symmetry, and a low-temperature metastable phase, martensite, with low symmetry. Although many variants of martensite can be formed from an austenitic single crystal, during the reverse transformation all the variants lead to the same parent phase. The variants have the same crystalline structure, and they only differ on the relative orientation.

When rapid cooling is applied to the material at a temperature where ß phase is stable, the resulting austenite is metastable. For lower temperatures, the metastable martensitic phase appears. Superelasticity is possible only if the austenite is metastable; so that stress-induced martensite can form. This requires the working temperature to be higher than A_f, the austenite finish phase transformation temperature. Initially, when loads are applied, metastable austenite is deformed elastically until the forward transformation stress (s_t) is attained, starting a non linear stress-strain relation afterwards. When unloading, the phase transformation reverses and the material recovers its original shape. In tensile tests, reversible non linear strains between 2 and 8% can be attained and energy dissipation occurs through hysteresis.

When the working temperature is increased, s_t also increases, because the parent phase is more stable. Above the limit temperature, M_D, pseudoelasticity is not possible due to austenite stability, Otsuka et al. Also there is a maximum strain above which strains are no longer reversible; this limit is lower for a polycrystalline material than for a single crystal. The grain size has an effect on the phase transformation temperatures and on the shape of the hysteresis cycles and, therefore, on the energy dissipation capacity.

Most of the previous research involves Ni-Ti alloys or Cu- and Fe-based alloys due to their potential or effective technological applications. Thorough reviews concerning potential uses of Ni-Ti based SMAs in earthquake engineering can be found in DesRoches and Smith, Song et al., and Wilson and Wesolowsky. They include state-of-the-art information about modelling, design and testing of devices, as well as analytical and experimental studies on their use in buildings and bridges.

This paper presents the results of a study on Cu-based shape memory alloy (SMA) elements for energy dissipation in connections under earthquake excitation. The elements include round bars for use as mechanical connectors and plates for ADAS-type energy dissipation devices. Two nominal compositions of CuZnAl were used. The study of both compositions in parallel was of interest because of the large energy dissipation capacity of one and the self-centering capability of the other. Both materials may be combined to optimize the behaviour of connections that include elements made of these alloys.

2. MATERIAL CHARACTERIZATION

The following two nominal compositions of CuZnAl were used as target: Cu 16.9wt%Zn 7.71wt%Al and Cu 20.36wt%Zn 5.2wt%Al. Figure 1 shows the relation between the composition and the M_s transformation temperature. A slight difference in composition produces large differences in M_s. After making several bucks, two alloys were selected to proceed with the fabrication of sample tests. Alloy A (Cu 17wt%Zn 7.2wt%Al) presented austenitic phase at room temperature, while alloy B (Cu 20.6wt%Zn 5.7wt%Al) presented martensitic phase at room temperature. Differential Scanning Calorimetry (DSC) tests gave the following phase transformation temperatures for alloy A: A_f = 22ºC, A_s = -5.2ºC, M_s = 4.9ºC, and M_f = -10.2ºC. For alloy B no phase transformation was observed when heating up to 100ºC. At room temperatures austenite and martensite phases were observed through optical metallographies.

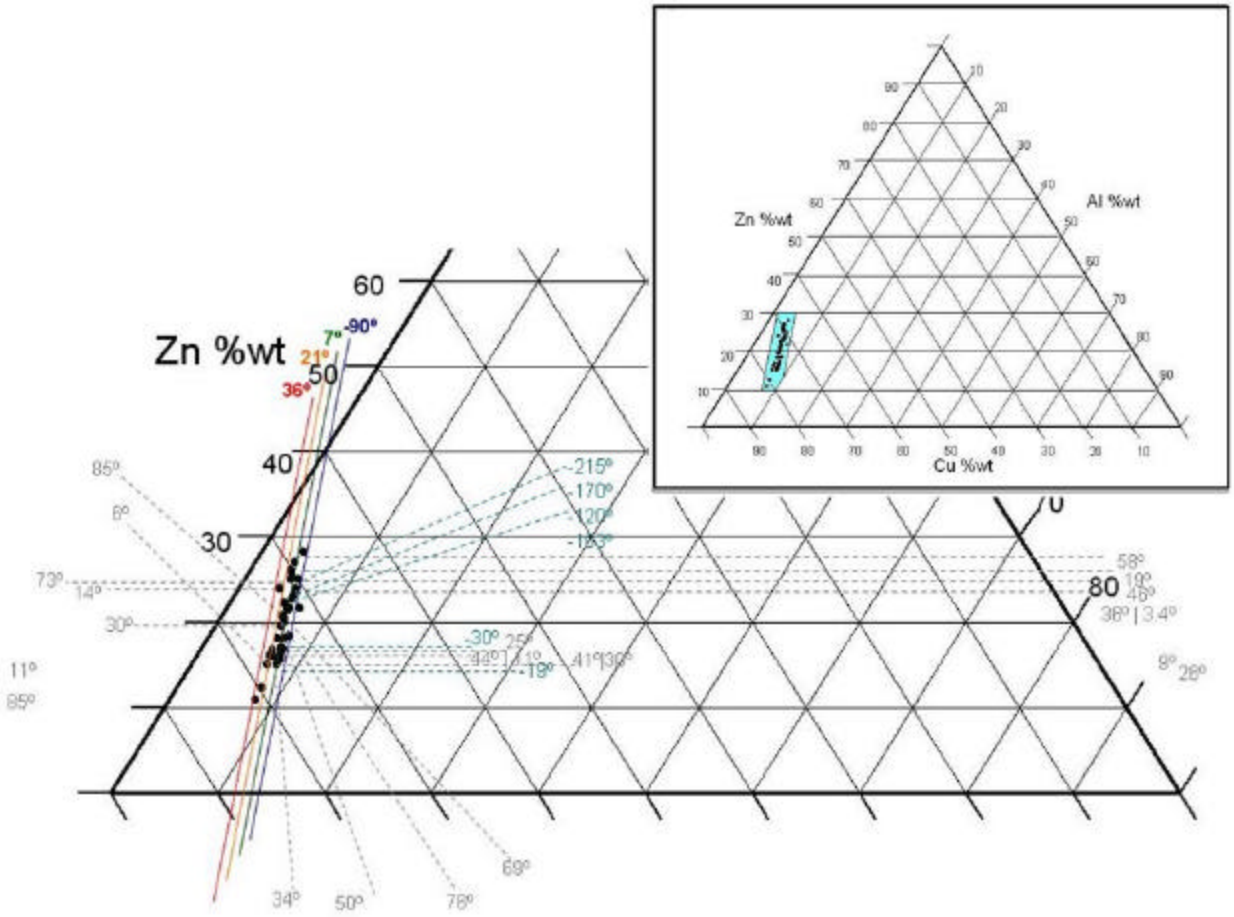

Figure 1. M_s variation as function of CuZnAl composition

3. BAR FABRICATION AND CHARACTERIZATION

Two types of thermo-mechanical treatments were used, alternatively, on alloy A to obtain round bars for material testing. The first treatment (TMT1) consisted of hot-rolling with a total of 50 to 60% reduction, imposed in two to four rolling passes at 850ºC and water quenching, followed by annealing at 800ºC for 10 min, and water quenching. The second treatment (TMT2) consisted of hot forging followed by extrusion with a 60% area reduction at 850ºC, and water quenching. For both treatments, no recristalization was observed and most of the grains remained with elongated shape.

Samples 7 cm long, of 3, 5 and 6.5 mm diameter were machined from the hot-rolled material and heated at 800ºC for 10 min. Static and cyclic tensile tests were performed at room temperature. The influence of strain amplitude, loading history and frequency (0.25 and 1 Hz) on the stiffness and equivalent viscous damping were studied for the dynamic case, (Saavedra).

Figure 2 shows stress-strain relationship for static and dynamic tests. For the static case, envelope curves obtained from cyclic tests performed at 1 Hz are also shown; only the 3 mm bar coincides for both type of tests, while for larger diameters the envelopes give lower stresses. Maximum stresses increased for the smaller diameter bars. Maximum strains attained were about 5-6%. The phase transformation stresses were 150 MPa, 50 and 30 MPa for the 3, 5 and 6.5 mm, respectively. In the cyclic tests superelasticity is apparent. The bar was slightly pre-tensioned.

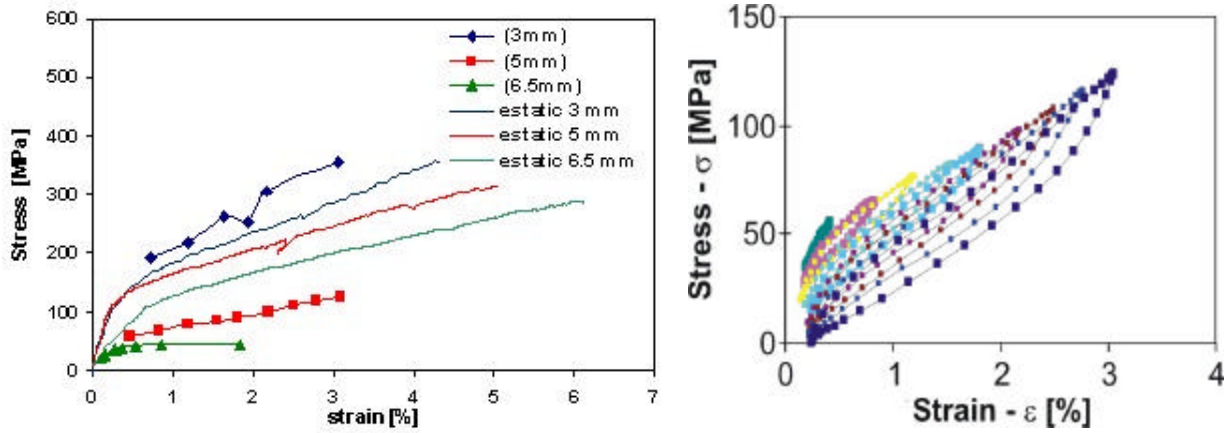

Static test, different bar diameters Cyclic test, 5 mm, 1 Hz, 18ºC

Figure 2 Stress-strain relationship; Hot rolled bar

Figure 3 shows the relationship between secant stiffness and equivalent viscous damping with strain amplitudes for the three diameter bars for tests performed at 0.25 and 1 Hz. The equivalent viscous damping was calculated as the energy loss per cycle divided by (4π maximum strain energy per cycle) and the secant stiffness as the maximum stress divided by the maximum strain attained.

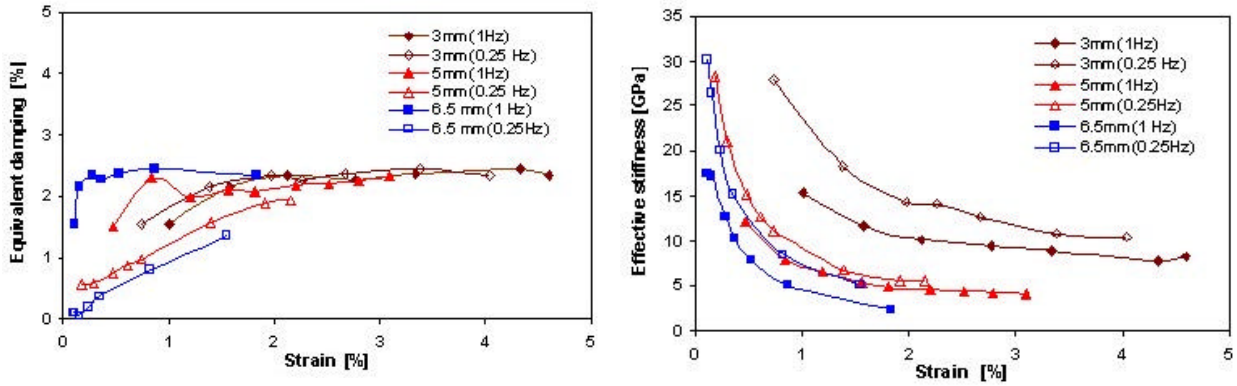

Equivalent damping Secant stiffness

Figure 3. Equivalent damping and secant stiffness for hot rolled bars.

Frequency affects equivalent damping values for low amplitude strains where calculations are less precise, but it has a larger influence on the secant stiffness calculation. One specimen was tested months later and a similar behavior than the previous one was observed.

Bars 10 cm long and 7 mm diameter were machined from the extruded material. Static and cyclic tensile tests were performed at three different temperatures: room, 25º and 50ºC. The influence of strain amplitude and temperature on the stiffness and equivalent viscous damping were studied for the dynamic case. During the tests, the surface temperature of the bars was measured by thermocouples, (Vera).

Figure 4 shows the stress-strain relationship for static and dynamic tests. Maximum stresses increased for higher temperatures tests. The maximum strains varied between 4.5 and 6.5%. Optical metallographies showed that the red line bar tested at 50ºC correspond to a bar that has a significant degree of grain recristalization as opposed to all the others, where grains maintained a predominantly elongated shape.

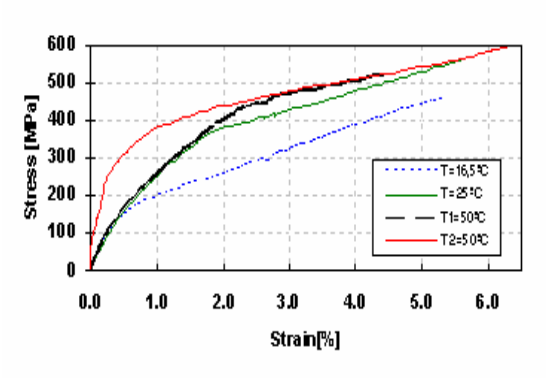

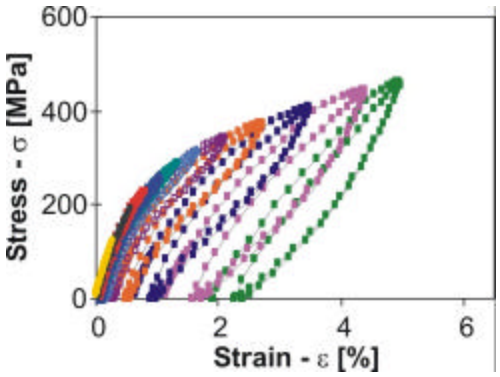

Static tests at different temperatures Cyclic tests, 7 mm, 1 Hz, 25ºC

Figure 4 Stress-strain relationship for extruded bars

Figure 5 shows the variation of equivalent damping and secant stiffness with strain amplitude and temperature. Again larger differences appeared for low strain amplitudes. The material temperature increased 6ºC during loading while it decreased to the controlled test temperature during unloading.

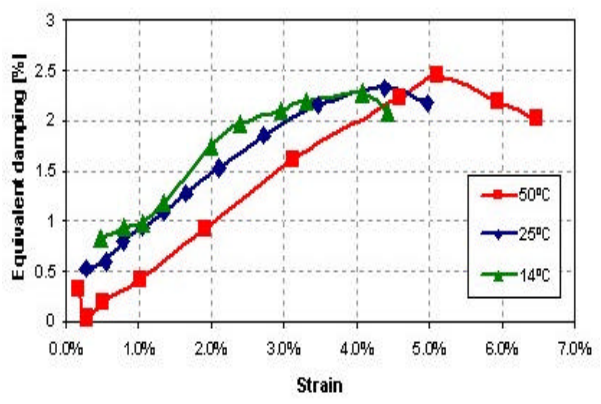

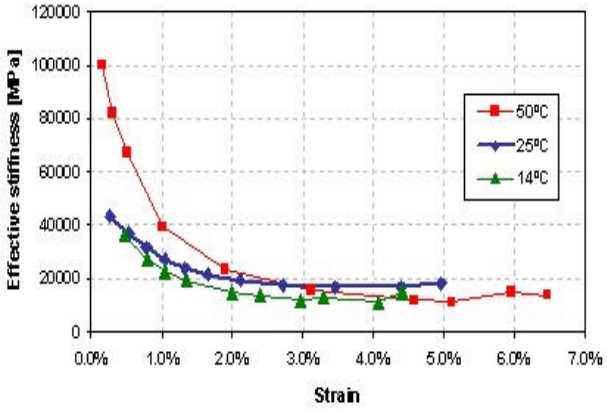

Equivalent damping Secant stiffness

Figure 5. Equivalent damping and secant stiffness for extruded bars.

Extruded bars attained higher maximum stresses and phase transformation stresses than hot-rolled bars. The superelastic strain limit, defined as the maximum strain at which the deformation is recovered completely upon load removal, was 3% for hot rolled bars, while for extruded bars it was 1% for tests performed at 50ºC, and 2.1% for the tests at other temperatures. Damping is low for both cases.

4. PLATE TESTING

Four ADAS shaped plates were fabricated through forging and hot rolling of alloy B. Table 1 shows plate dimensions, phase transformation stresses and Young Module obtained from tensile tests of 3 mm diameter rod taken from material of each plate. Values are quite different because each plate was made from a different cast. Based on the previous properties, V_y and Δ_y were predicted analytically, (Vargas).

Figure 6 shows the test setup, similar to the one used by Esguerra. Incremental amplitude displacement cycles up to 40 mm were applied at 0.088 Hz; a sine-wave signal was used during the testing program. Instrumentation included strain gages at the center of each plate and a load cell and a LVDT to record the overall load-deflection response.

Table 1 Plate dimensions and mechanical properties

Plate	h [mm]	b [mm]	t [mm]	σ_t [MPa]	E [MPa]	V_y [ton]	Δ_y [mm]
1	148	75	9.5	208.3	48000	0.32	5.00
2	148	75	9.2	151	37000	0.22	4.84
3	146	60	8.3	143.8	43400	0.13	4.25
4	150	56	8.3	118.8	43200	0.10	3.73

Figure 6 Testing device for ADAS type plate

Figure 7 shows the total vertical force vs the relative displacement under cyclic loading for plates 1 and 2. These curves are quite different from those obtained for steel or pure copper ADAS plate. Yield strength and yield displacement are not easily defined, but are of the same order than the analytical values shown in Table 1. Strain-hardening is apparent. The behavior of ADAS elements is stable and they dissipate energy in a non-degradable manner. Equivalent damping was about 8% for displacements between 30 to 35 mm. Slight permanent deformations could be observed after the test, as can be seen in figure 8, however, the plates recovered part of these deformations with time.

Theoretically, moment, curvature and strain ε_x at the center of the plate should be zero. However, strain gage measurements showed that ε_x increased with increased displacements. This indicates the existence of axial tension during large displacement cycle due to membrane action. In addition, lateral movement at the bearing was also observed, making the double clamped boundary condition assumed initially, unrealistic.

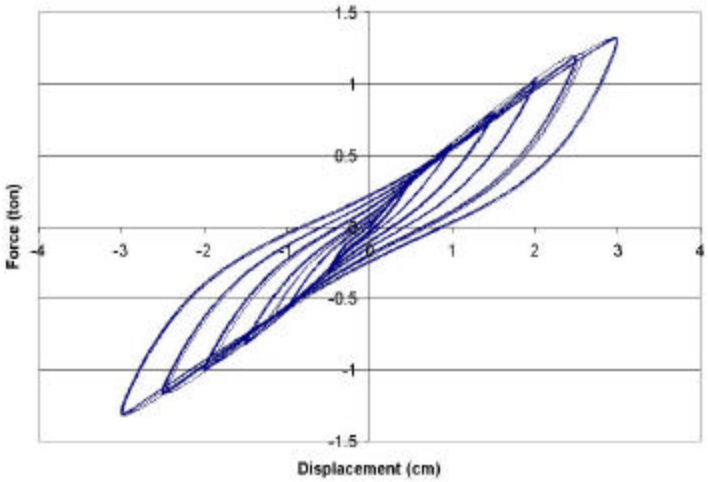

Figure 7 Force-displacement relationship

Figure 8, permanent deformation after 40 mm out of plane displacement

5 CONCLUSION

Bars of different diameters were fabricated from alloy A using extrusion and hot-rolling. The mechanical properties (stiffness, martensitic transformation stress, tensile strength, ultimate strain) and equivalent damping of these bars were experimentally determined and their dependency on type, amplitude and frequency of excitation, and operating temperature was studied. Young's modulus varied from 40 to 50 GPa. Extruded bars attained higher maximum stresses and transformation stress limits than hot-rolled bars, showing an increase in maximum stress for higher temperatures, while hot-rolled bar maximum stresses increased for the smaller diameter bars. Ultimate strains varied between 4.5 and 6.5%. The superelastic strain limit was 3% for hot-rolled bars while for extruded bars it was 1% and 2.1%, for tests performed at 50ºC and at other temperatures, respectively. In both cases, equivalent damping increased and secant stiffness decreased with larger strains, attaining a maximum value of 2.5% damping. Extruded bars were stiffer than hot-rolled bars, and stiffness diminished for higher frequencies.

In addition, four annealed martensite plates (15x12x1 cm) made from alloy B of equal bending strength shape were tested under cyclic out-of-plane flexure. Stable cycles and limited residual deformations were observed up to 20% drift. Equivalent damping ratio increased with larger drift, reaching a maximum of 8% for a 20% drift.

ACKNOWLEDGEMENTS

The authors gratefully acknowledge the financial support of CONICYT, Chile, through FONDECYT grants 1030554 and 1070370. The important contributions of Eng. Pedro Soto from Universidad de Chile, Carl Luders from PUC and Gabriel Palma from the Ministry of Public Works (MOP) are also recognized.

REFERENCES

DesRoches, R. and Smith, B. (2004) Shape Memory Alloys in Seismic Resistant Design and Retrofit: A Critical Review of their Potential and Limitations. *Journal of Earthquake Engineering*, **8:3**, 415-429.
Esguerra, C. (2003), Análisis y diseño de estructuras con disipadores metálicos de cobre. Magíster en Ciencias de la Ingeniería Thesis, Pontificia Universidad Católica.
Otsuka K. and Wayman C.M. (1998) eds. Shape Memory Materials. Cambridge University Press, Cambridge.
Saavedra A. (2007) Caracterización del Comportamiento de una aleación CuZnAl en Probetas Laminadas. *Civil Engineering Thesis*, Universidad de Chile
Song, G. Ma, N., and Li, H., (2006), Applications of Shape Memory Alloys in Civil Structures, *Engineering Structures*, **28:9**, 1266-1274.
Vargas J. (2007) Ensayo de placas ADAS de láminas de CuZnAl, *Civil Engineering Thesis, Universidad de Chile*

Vera A. (2007) Caracterización de una aleación Superelástica CuZnAl Extraída, Considerada para Disipadores de Energía Sísmica. *Mechanical Engineering Thesis*, Universidad de Chile.
Wilson, J.C. and Wesolowsky, M.J. (2005), Shape Memory Alloys for Seismic Response Modification: A State-of-the Art Review. *Earthquake Spectra*, **21: 2**, 569-601.